hemingway is required for sperm flagella assembly and ciliary motility in *Drosophila*

Fabien Soulavie[a], David Piepenbrock[b], Joëlle Thomas[a], Jennifer Vieillard[a], Jean-Luc Duteyrat[a], Elisabeth Cortier[a], Anne Laurençon[a,*], Martin C. Göpfert[b], and Bénédicte Durand[a]

[a]Centre de Génétique et de Physiologie Moléculaire et Cellulaire, UMR 5534, Centre National de la Recherche Scientifique, Université de Lyon 1, 69622 Lyon, France; [b]Department of Cellular Neurobiology, University of Göttingen, 37077 Göttingen, Germany

ABSTRACT **Cilia play major functions in physiology and development, and ciliary dysfunctions are responsible for several diseases in humans called ciliopathies. Cilia motility is required for cell and fluid propulsion in organisms. In humans, cilia motility deficiencies lead to primary ciliary dyskinesia, with upper-airways recurrent infections, left–right asymmetry perturbations, and fertility defects. In *Drosophila,* we identified *hemingway* (*hmw*) as a novel component required for motile cilia function. *hmw* encodes a 604–amino acid protein characterized by a highly conserved coiled-coil domain also found in the human orthologue, KIAA1430. We show that HMW is conserved in species with motile cilia and that, in *Drosophila*, *hmw* is expressed in ciliated sensory neurons and spermatozoa. We created *hmw*-knockout flies and found that they are hearing impaired and male sterile. *hmw* is implicated in the motility of ciliated auditory sensory neurons and, in the testis, is required for elongation and maintenance of sperm flagella. Because HMW is absent from mature flagella, we propose that HMW is not a structural component of the motile axoneme but is required for proper acquisition of motile properties. This identifies HMW as a novel, evolutionarily conserved component necessary for motile cilium function and flagella assembly.**

Monitoring Editor
Julie Brill
The Hospital for Sick Children

Received: Oct 24, 2013
Revised: Jan 27, 2014
Accepted: Feb 10, 2014

INTRODUCTION

Cilia and flagella are microtubular structures that are highly conserved across eukaryote species. They are found from unicellular microalgae to complex metazoans, where they play major functions in physiology and development. In humans, cilia dysfunctions are responsible for several diseases called ciliopathies (Hildebrandt *et al.*, 2011; for review see Drummond, 2012). Cilia are defined by a skeleton of nine microtubule doublets—the axoneme—which is assembled from the centriole/basal body. Cilia are routinely classified as motile cilia or sensory/primary cilia based on their motile properties and the architecture of the axoneme. Most motile cilia are composed of nine peripheral doublets plus a central pair of microtubules—the 9+2 cilia. Sensory/primary cilia are generally composed of nine peripheral doublets of microtubules and are called 9+0 cilia. Most 9+0 cilia are immotile; however, 9+0 motile cilia can be found in the mammalian embryonic node (McGrath and Brueckner, 2003). Another example is the mechanosensory cilium of *Drosophila* auditory sensory neurons. Hearing in *Drosophila* is mediated by the Johnston's organ (JO), a chordotonal stretch receptor organ located in the fly's antenna (Kamikouchi *et al.*, 2009). JO comprises ~500 ciliated mechanosensory neurons with 9+0 axonemes (Kamikouchi *et al.*, 2006). Approximately half of these neurons are auditory neurons, and the other half monitor gravity and wind. Auditory neurons serve dual, transducing and actuating roles, converting sound-induced vibrations of the antenna into electrical responses and actively assisting the vibrations that they transduce (Göpfert and Robert, 2003; Effertz *et al.*, 2011). This neuronal motility seems to involve axonemal dynein motors (Göpfert and Robert, 2003; Senthilan *et al.*, 2012), and, judging from electron microscopy, the sensory cilia of JO neurons are endowed with dynein-like arms (Kavlie *et al.*, 2010).

This article was published online ahead of print in MBoC in Press (http://www.molbiolcell.org/cgi/doi/10.1091/mbc.E13-10-0616) on February 19, 2014.

*Present address: Laboratoire de Biologie Moléculaire de la Cellule, UMR 5239, Centre National de la Recherche Scientifique, Ecole Normale Supérieure de Lyon, Université de Lyon 1, 69364 Lyon, France.

Address correspondence to: Bénédicte Durand (benedicte.durand@univ-lyon1.fr).

Abbreviations used: CBY, CHIBBY; GFP, green fluorescent protein; hmw, hemingway; JO, Johnston's organ; RFX, regulatory factor X; TTLL, tubulin tyrosine ligase–like.

Dynein arms are observed in all motile 9+0 or 9+2 cilia and ensure motility (Satir, 1989). Cilia motility also requires several components that are conserved throughout evolution. The 9+2 cilia show radial spokes and nexin links not observed in 9+0 motile cilia such as nodal cilia or *Drosophila* chordotonal cilia. These differences likely reflect the distinct movements generated by the two types of motile cilia: either rotational or waveform movements. Studies designed to identify proteins involved in cilia and flagella motility found that >64 proteins likely account for the specification of motile cilia (Avidor-Reiss *et al.*, 2004; Baron *et al.*, 2007).

In addition to dyneins, cilia motility involves C-terminus tubulin posttranslational modifications. Among tubulin posttranslational modifications, glycylation and glutamylation have been demonstrated to play a role in cilia motility. The enzymes responsible for glycylation or glutamylation belong to the tubulin tyrosine ligase–like (TTLL) family. Polyglutamylations modulate cilia motility (Gagnon *et al.*, 1996; Ikegami *et al.*, 2010; Kubo *et al.*, 2010; Suryavanshi *et al.*, 2010). For instance, the lack of polyglutamylation enzymes TTLL6 and TTLL9 in *Tetrahymena thermophila* and in *Chlamydomonas reinhardtii*, respectively, results in completely immotile flagella (Kubo *et al.*, 2010; Suryavanshi *et al.*, 2010) due to misregulation of inner dynein arms. Furthermore, asymmetric bending of cilia in mice respiratory airways is affected when the polyglutamylation enzyme TTLL1 is lost (Ikegami *et al.*, 2010). However, tubulin modification defects also lead to axonemal instability (Wloga and Gaertig, 2010; O'Hagan *et al.*, 2011). In *Drosophila melanogaster*, tubulin modifications are essential for sperm axonemal integrity (Hoyle *et al.*, 2008). Decreasing the levels of TTLL6b by RNA interference (RNAi) results in structural defects in axonemal architecture (Rogowski *et al.*, 2010), showing that tubulin modifications can have consequences for both axonemal stability and motility.

RFX transcription factors play a critical function in controlling genes required for cilia assembly (Swoboda *et al.*, 2000; Dubruille *et al.*, 2002; Bonnafe *et al.*, 2004; Rogowski *et al.*, 2009; Thomas *et al.*, 2010). In a screen for RFX target genes in *Drosophila* (Laurençon *et al.*, 2007), we identified *CG7669* (which we call *hemingway* [*hmw*]; see later discussion), which is associated only with species harboring motile cilia. We show that, in *Drosophila*, *hmw* is expressed only in cells harboring motile cilia, namely type I ciliated neurons of the chordotonal organs and in male germline cells. HMW protein is found in the cytoplasm and in ciliary endings of sensory cilia and in the germ cell cytoplasm from spermatocytes to late spermatids. HMW is lost at the onset of sperm individualization, and no HMW protein is found in mature spermatozoa. *hmw*-null flies show auditory defects and male sterility. In the antennae, *hmw* is required for the active amplification of sound-induced antennal vibrations by auditory neuron cilia, documenting that the motility of these cilia requires *hmw*.

In elongating spermatids, HMW is critical for axonemal elongation and integrity. Spermatid individualization defects and aberrant tubulin modifications of the axoneme are observed in *hmw*-mutant testes. Taken together, our results demonstrate that in *Drosophila*, HMW is required for axonemal integrity in the testis and for sensory cilia motility, indicating that HMW is a novel actor controlling motile cilia physiology.

RESULTS

The RFX target gene *hmw* is specific for ciliated species

In a screen for *Drosophila* genes containing an RFX binding site in their promoter, *CG7669*/*hmw* was identified as a potential RFX target (Laurençon *et al.*, 2007). HMW protein is composed of 604 residues with a conserved domain located in the C-terminus. This conserved domain of unknown function is also found in the human orthologue, KIAA1430, and is referred to as the KIAA1430 domain in the Pfam database (Figure 1A). The *Drosophila* domain shares only 31% identity with the human KIAA1430 domain and 24% with the one found in *C. reinhardtii*. Structural predictions based on the DSC algorithm (King *et al.*, 1997), however, suggest a strong conservation of the secondary structure, with two helices separated by a spacer (Figure 1B) that belongs to the family of coiled-coil domains. Outside the coiled-coil domain, the HMW proteins of different species do not show high conservation.

In vertebrates, insects, and *C. reinhardtii,* the KIAA1430 domain is located in the C-terminal part of the protein. Conversely, the KIAA1430 protein domain in other bikonts is located in their N-terminus (Figure 1A). Although the overall sizes of the proteins are very different between species, the sizes of the different KIAA1430 domains are similar, ranging from 71 residues in *Toxoplasma gondii*, *Giardia intestinalis*, and *Phytophthora infestans* to 96 residues in *T. thermophila*. In metazoans, domain size varies from 73 residues in humans to 83 in *D. melanogaster*. Furthermore, prediction of the ternary structure showed that the KIAA1430 domain is located at the periphery of the protein in *Drosophila* and humans (unpublished data). This may indicate a possible important role of this domain in protein function. Of interest, only one protein containing this domain is detected in ciliated species harboring motile cilia. The KIAA1430 human protein was found in the proteome of airway motile cilia (Ostrowski *et al.*, 2002) and corresponds to flagella-associated protein 97 in *C. reinhardtii* (Merchant *et al.*, 2007). In addition, no protein containing the KIAA1430 domain could be found in *Caenorhabditis elegans* that does not harbor motile cilia (Figure 1C), suggesting specific association with motile cilia.

hmw is exclusively expressed in ciliated cells in *Drosophila*

To detect *hmw* expression in *Drosophila*, we created transgenic flies expressing an HMW–green fluorescent protein (GFP) fusion protein under the control of the *hmw* promoter. We observed HMW-GFP in sensory neurons at all stages of development. HMW-GFP was restricted to the chordotonal organs of embryos (Figure 2, A and B) and pupae antennae (Figure 2D). HMW-GFP was found in the cell body and the ciliated ending, also called outer dendritic segment, at the tip of the dendrite (Figure 2B). Of importance, we did not detect HMW-GFP in external sensory organs (Figure 2, les and ves) that have nonmotile cilia, as observed in embryos (Figure 2A). In an *Rfx*-mutant background, *hmw* expression was lost, confirming that, in the peripheral nervous system, *hmw* is regulated by RFX (Figure 2C).

hmw expression was also detected in adult testis, where HMW-GFP labeling was found at various stages, ranging from spermatocytes to elongating spermatids (Figure 3). In spermatocytes, the protein was observed in the entire cell body (Figure 3A and Supplemental Figure S1). During spermiogenesis, the protein was maintained in the cell body of elongating spermatids (Figure 3, B–D, and Supplemental Figure S1) but was absent from spermatids at the onset of individualization (unpublished data). Of interest, HMW-GFP did not colocalize with basal bodies stained with anti–γ-tubulin (Figure 3A) or very weakly stained flagellar components as revealed by acetylated α-tubulin staining of the axonemes (Figure 3, B–D, and Supplemental Figure S1). In the absence of the endogenous protein, that is, in the rescue strain in which HMW-GFP was expressed in an HMW-deficient background (Supplemental Figure S1), HMW was also observed predominantly in the cytoplasm from spermatocytes to elongating spermatids but was not detectable above background staining levels in spermatozoids (Supplemental Figure S1). Together

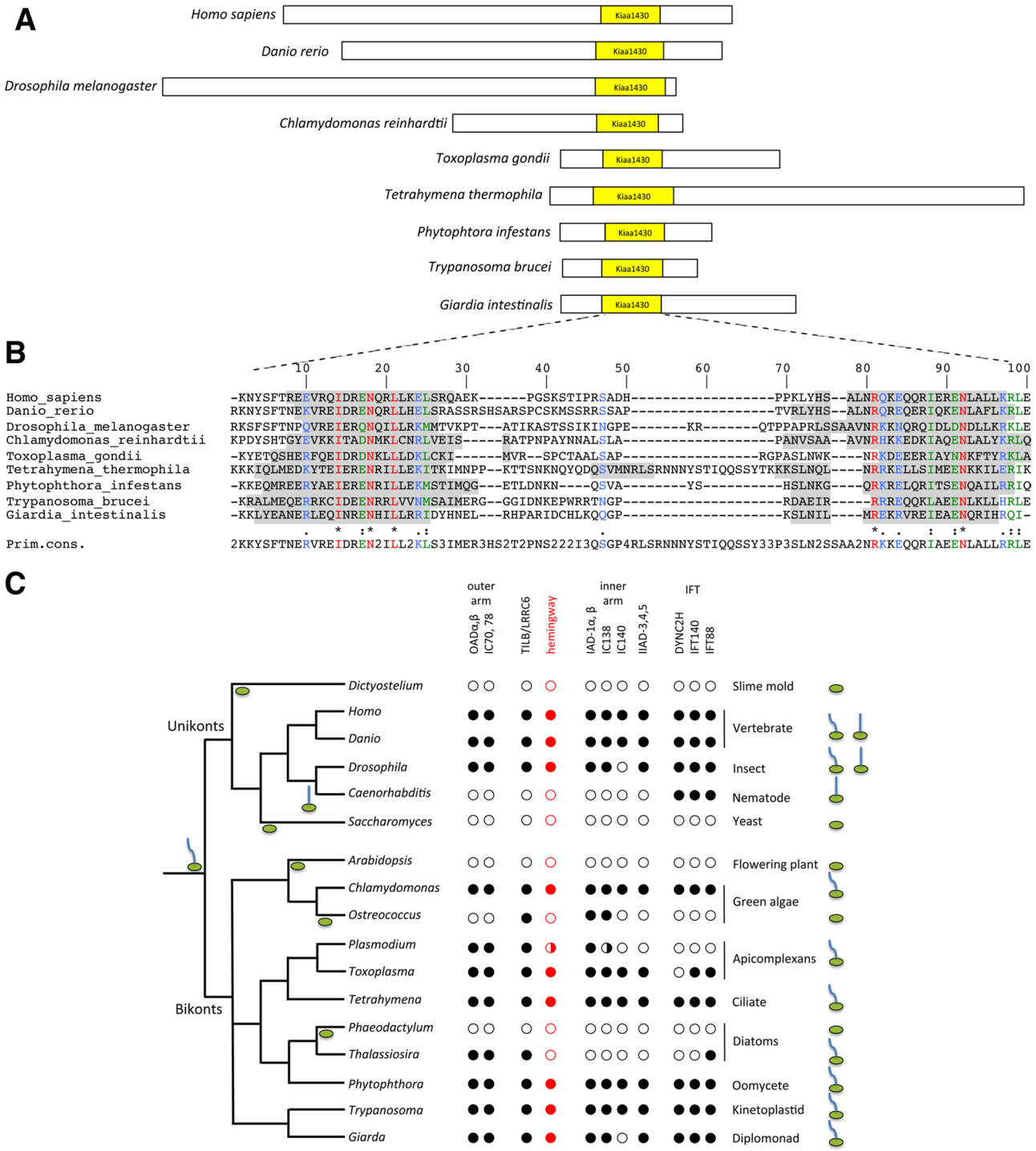

FIGURE 1: KIAA1430 is a conserved domain within motile ciliated species. (A) Schematic representation of KIAA1430 domain containing proteins in a set of ciliated species. KIAA1430 domain is shown in yellow. *Homo sapiens*, KIAA1430; *Danio rerio*, zgc:85910; *D. melanogaster*, CG7669; *C. reinhardtii*, FAP97; *T. gondii*, EEE19087; *T. thermophila*, TTHERM_00069200; *P. infestans*, XP 002905569.1; *Trypanosoma brucei*, XP_822891; *G. intestinalis*, GL50581_606. (B) ClustalW Multiple protein alignment of KIAA1430 domain sequences of the proteins in A. Secondary structure was predicted by the DSC (King *et al.*, 1997) model. Gray, predicted helix structures. Blue, weakly similar amino acids; green, strongly similar; red, identical. Primary consensus refers to the most represented amino acid for each position; numbers are given when several amino acids are equally represented. (C) Phylogenetic tree showing KIAA1430 domain–containing proteins in several eukaryotic species (adapted from Wickstead and Gull, 2007). Schemes on the right indicate whether motile cilia and/or immotile cilia are found in each species. Filled circles, KIAA1430 protein is present; empty circles, no orthologues; half-filled circles, only very distant components can be identified. Black, conserved components of the cilia motility machinery, outer and inner dynein arms, and conserved components of the intraflagellar transport machinery (Kavlie *et al.*, 2010).

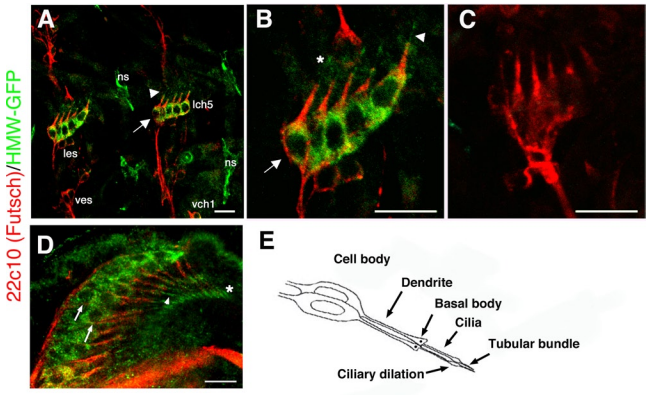

FIGURE 2: Distribution of HMW in the *Drosophila* peripheral nervous system. (A–D) Immunolabeling of HMW-GFP in sensory neurons labeled in red with 22C10 antibody (anti–Futsch protein). HMW-GFP is detected by an anti-GFP antibody. (A) In embryonic abdominal segments, HMW-GFP is detected only in chordotonal neurons and not in external sensory neurons. HMW-GFP is found both in the cell body (arrow) and in the ciliated endings (arrowheads). (B) Magnification of a group of lateral chordotonal organs 5 from A, showing stronger accumulation at the level of the ciliary dilation (asterisks). (C) No HMW-GFP is detected in *Rfx*-deficient flies. (D) In the adult second antennal segment, HMW-GFP is detected in the chordotonal neurons of the Johnston's organ, the cell body (arrow), and the cilia (arrowhead). Anti-Futsch labels only the cell body and the dendrite. (E) Schematic representation of two chordotonal neurons typically found in one sensilla in the Johnston organ. lch5, lateral chordotonal organ; vch1, ventral chordotonal organ 1; les, lateral external sensory organ; ves, ventral external sensory organ. ns, nonspecific staining of the GFP antibody. Scale bars, 10 µm.

the results show that in *Drosophila*, HMW-GFP is only expressed in cells that harbor motile cilia: the chordotonal neurons and the male germ cells.

hmw is required for mechanical amplification in the *Drosophila* ear

To understand the precise function of HMW, we constructed a null hmw^{1} mutation, using homologous recombination (Maggert *et al.*, 2008). As shown in Figure 4A, most of the *hmw* coding region is deleted from the recombinant construct. PCR performed with primers shown in Figure 4A confirmed that the recombination occurred correctly on the left and right arms of the construct and that *hmw* sequences are deleted in the hmw^{1} allele (Supplemental Figure S2). In addition, we sequenced the entire recombinant loci to verify that the 3′ untranslated region of *CG7670* was unaffected in hmw^{1} allele. By reverse transcription-PCR we showed that no *hmw* mRNAs were detectable and that mRNA expression from the partially overlapping gene *CG7670* was unaffected (Supplemental Figure S2). $hmw^{1/1}$ mutant flies were viable and developed in Mendelian proportions up to adulthood, showing that *hmw* is not required for survival during development. Because chordotonal cilia are required for fly gravitaxis, hearing, and coordination, we first assessed fly behaviors using a bang assay: wild-type flies in a tube move rapidly upward on vertical surfaces, whereas flies with defective chordotonal organs stay at the bottom of the tube (Jarman *et al.*, 1993). However, $hmw^{1/1}$ mutant flies did not present significant behavioral differences when compared with control and rescue flies (unpublished data), indicating that coordination and gravitaxis are not significantly impaired in $hmw^{1/1}$ mutants.

To test more directly whether *hmw* is implicated in chordotonal organ function, we analyzed sound responses of the fly JO (Figure 4, B and C). To evoke sound responses, we exposed the flies to pure tones of different intensities at the best frequency of their antennal sound receiver (Göpfert *et al.*, 2006). Mechanical and electrical responses of JO neurons were assessed by recording sound-induced antennal displacements and sound-evoked potentials from the antennal nerve (Göpfert *et al.*, 2006). In w^{1118} controls, sound particle velocities of ~40 mm/s sufficed to evoke electrical responses. The antennal displacement response displayed the characteristic compressive nonlinearity that, resulting from the motility of auditory JO neurons, amplifies the antenna's displacement response to low-intensity sounds with an amplificatory gain of ~10 (Effertz *et al.*, 2011). In $hmw^{1/1}$ mutants, the sound particle velocities required to evoke nerve responses were increased to ~70 mm/s, and the amplification gain provided by the motility of JO neurons was reduced to ~5. The amplification gain was partly restored when we expressed *hmw-gfp* in the $hmw^{1/1}$ mutant background, and sound particle velocities required to evoke nerve potentials were restored to 40 mm/s, as observed in w^{1118} and *hmw-gfp* controls. Hence HMW is required for sensitive sound responses and proper mechanical amplification by auditory JO neurons, indicating that ciliary force generation by these neurons depends on HMW. Because of these hearing defects, we named *CG7669* after Ernest Hemingway, *hmw*, who suffered from hearing loss toward the end of his life.

To understand how HMW could act on cilia motility, we analyzed the ultrastructure of JO neuron cilia by electron microscopy. We did not observe ultrastructural defects in $hmw^{1/1}$ mutant flies. In particular, dynein-like arms were still present (Figure 5). Thus *hmw* seems not required for sensory cilia assembly but is for proper sensory cilia function.

hmw is required for axonemal elongation and maintenance during *Drosophila* spermatogenesis

$hmw^{1/1}$ mutant flies were viable, but males were completely sterile, whereas female fertility appeared normal. We observed a complete absence of mature spermatozoa in the seminal vesicles from $hmw^{1/1}$ flies compared with controls (Figure 6, A and B). Male sterility was rescued by adding two copies of the reporter *hmw-gfp*, which restored mature spermatozoa in the seminal vesicles (Figure 6C). HMW is thus required for spermatogenesis in flies.

We performed tubulin staining of the testis (Figure 6, D–F) and observed that flagella and elongated spermatid cysts are still present in $hmw^{1/1}$ mutants (Figure 6E). Electron microscopy of $hmw^{1/1}$ mutant testis, however, revealed severe defects of the spermatid cysts (Figure 7). Whereas we always found all of the 63–64 major mitochondria derivatives in all cysts, axonemes were absent from most of the spermatids (Figure 7A). Examples of several axoneme defects found at different stages of cysts are shown in Figure 7, B–D. In early and intermediate cysts, we found that only 13.6 and 13.5% of the axonemes were intact, respectively ($n = 318$), whereas 14.2 and 14.1% of the axonemes were affected partially and the remnant 72.3 and 72.4% of the axonemes were entirely lost (Figure 7E). In mature cysts, most of the axonemes were missing or severely distorted (97.6%; $n = 126$), and almost no intact axoneme could be observed, indicating that although some axonemes can be assembled correctly in $hmw^{1/1}$ mutant flies, their stability is severely impaired, leading to complete breakdown during spermatid maturation.

Besides axonemal stability, flagellar elongation defects could contribute to the observed testis phenotype. To test this possibility, we monitored markers of axonemal elongation during spermatid

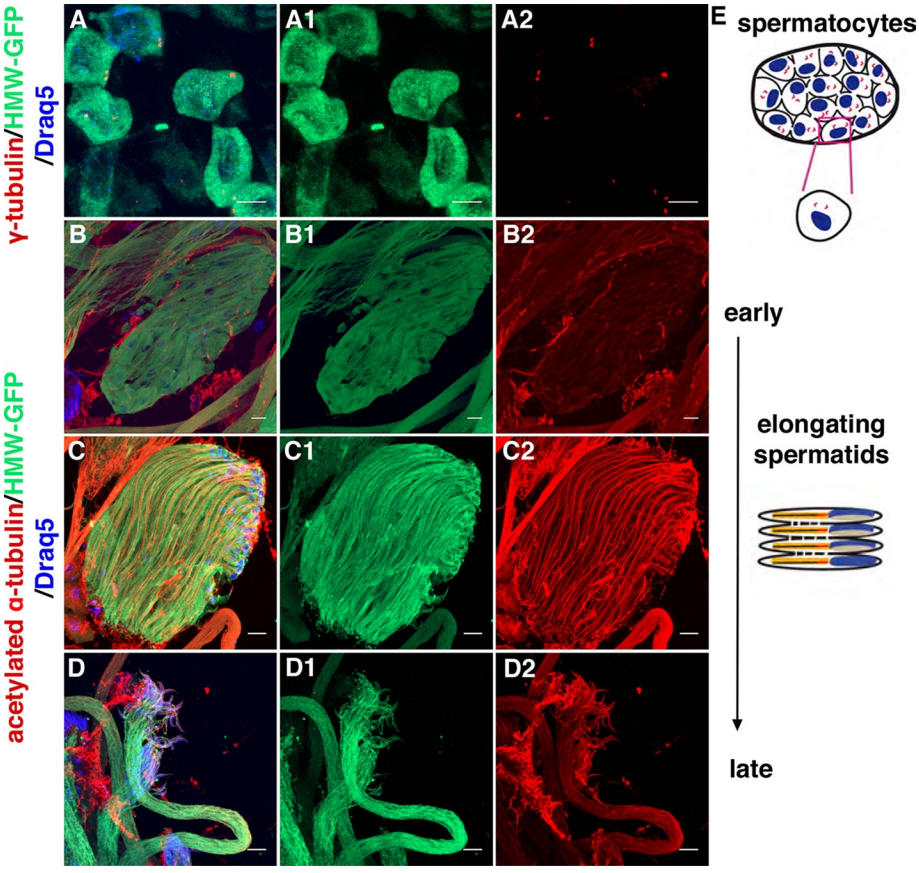

FIGURE 3: Expression pattern of HMW in *Drosophila* germ cells. (A) Spermatocytes from a 16-cell cyst. Centrioles/basal bodies are labeled with anti–γ-tubulin antibody (red). HMW-GFP is stained with anti-GFP antibody (green). Nuclei are labeled with Draq5 (blue). Single green (A1) and red (A2) channels are presented separately. HMW-GFP is localized in the cell body and does not colocalize with basal bodies. Scale bars, 10 μm. (B–D) Spermatids from 64-cell cysts. Three steps of spermatid elongation are shown: an early step when elongation starts, an intermediate state, and an almost fully elongated state. Anti–acetylated α-tubulin antibody (red) labels axonemal and mitochondria-associated microtubules. HMW-GFP is stained with anti-GFP antibody (green). Nuclei are labeled with Draq5 (blue). Single green (B1–D1) and red (B2–D2) channels are presented separately. As in spermatocytes, HMW-GFP is localized in the cell body during the three elongating steps. Scale bars, 10 μm. (E) Schematic representation of spermatogenesis steps. Top, 16-cell cyst, after two rounds of mitosis. Bottom, spermatid elongation steps after meiosis.

differentiation. CBY, for example, is a protein required for basal body maturation in *Drosophila* spermatocytes. CBY is maintained at the tip of the growing axoneme during spermatid differentiation, while nuclei remain tightly associated with the base of the axoneme (Enjolras *et al.*, 2012). As a consequence, nuclei and CBY are localized at the opposite poles of the growing cysts and separated by the axoneme in elongating spermatid cysts (Figure 8A). In *hmw*$^{1/1}$ mutants, we observed that in early elongating spermatid cysts, some CBY dots appear in the middle of the cysts and not only at their distal ends as seen in controls (Figure 8B). Nuclei also appeared mislocalized in *hmw*$^{1/1}$ cysts compared with controls, as they did not all cluster at the proximal side of the cysts. In late-elongating cysts, these defects in axonemal elongation were even more pronounced (Figure 8, C and D). In controls, clusters of nuclei were localized at one end of the cyst, and CBY dots appeared at the opposite distal end, whereas in *hmw*$^{1/1}$ mutants, nuclei and CBY dots were scattered all along the cysts (Figure 8, C and D, arrows and arrowheads, respectively). These observations indicate that in each cyst of *hmw*$^{1/1}$ testes there is variability in the length of the axonemes.

Together these data show that HMW is required both for axonemal elongation and integrity during spermiogenesis.

Tubulin modification pattern is affected in *hmw*$^{1/1}$ mutant flies

Electron microscopy indicated that spermatid individualization was also strongly affected in *hmw*$^{1/1}$ mutant testes (Figure 7A). Sperm individualization is a process by which spermatozoa separate from a 64-spermatid *syncytium* through plasma membrane remodeling by so-called individualization complexes. Theses complexes are composed of actin cones, which assemble around the spermatid nuclei and then synchronously move toward the tips of the flagella, removing all cytoplasm and organelles in the form of a waste bag and producing 64 individual sperms that are wrapped by their own membranes. To follow the individualization process, we analyzed the individualization of actin cones during spermatid elongation by staining F-actin with phalloidin (Figure 9). Whereas all F-actin cones assembled and progressed together in control flies, actin cones still assembled in *hmw*$^{1/1}$ mutants, but their progression was blocked, and the cones were dispersed inside the cysts (Figure 9, A and B). These observations show that even if individualization can initiate, it does not proceed throughout completion in the mutants, leading to empty seminal vesicles at the end of spermatogenesis.

Because individualization defects, as observed here in *hmw*$^{1/1}$ mutants, also characterize flies defective for tubulin modification (Rogowski *et al.*, 2009, 2010), we analyzed tubulin modifications in *hmw*$^{1/1}$ flies. The dynamics of tubulin modification is only partially described in *Drosophila* testes. Hence we first determined the dynamics of tubulin glutamylation (GT335 antibody; Wolff *et al.*, 1992) and monoglycylation (TAP952 antibody; Wolff *et al.*, 1992) or polyglycylation (Axo49 antibody; Bré *et al.*, 1996), together with detyrosination (anti–Glu-Tub antibody), during spermatogenesis. Glutamylated tubulin was observed during early flagella elongation and was maintained after individualization (Supplemental Figure S3, A and B). Detyrosinated tubulin was observed as soon as the axoneme elongated (Supplemental Figure S3) but was no longer detectable after sperm individualization. By contrast, monoglycylated tubulin appeared only on fully elongated spermatids (Figure 9C), and polyglycylation was observed only on the onset of sperm individualization (Figure 9E). Hence detyrosination and polyglycylation of tubulins were not observed concomitantly in wild-type cysts (Figure 9).

In *hmw*$^{1/1}$ *Drosophila* testes, glutamylated tubulin appeared normally distributed along the elongating spermatid axonemes compared with controls (Supplemental Figure S3B). However, in *hmw*$^{1/1}$ mutant testes, we observed that polyglycylated tubulin and detyrosinated tubulin appeared simultaneously in the axonemes (Figure 9F). In addition, the glycylation pattern in mutant testes

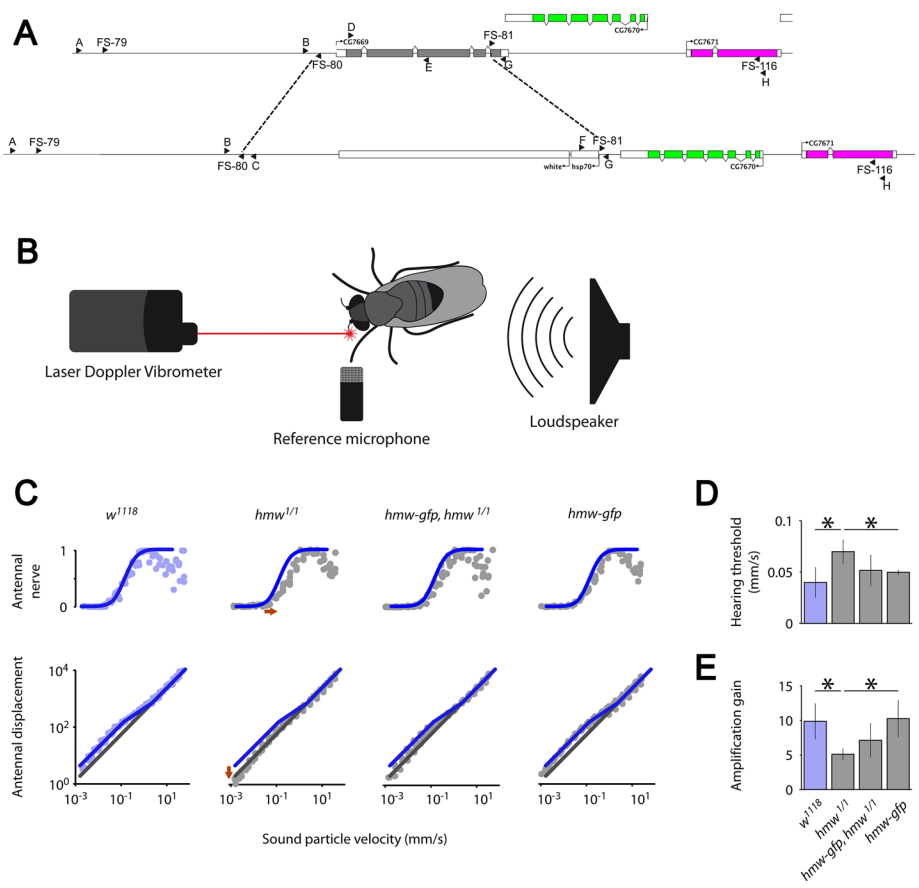

FIGURE 4: Auditory organ sound responses in controls and mutants. (A) Construction of *hmw*^{1} mutant allele. A white marker gene replaced the region between FS-80 and FS-81 primers. Primers A–C and F–H are designed to amplify the left and right recombinant loci, respectively. Primers D and E amplify *CG7669* locus in wild-type but not *hmw*$^{1/1}$ homozygous mutant. Primers B–G allow amplification of a 2-kb product in wild type, a 4.9-kb product in *hmw*$^{1/1}$, and both in heterozygous flies. The remaining fifth exon of *CG7669* is noncoding. (B) Scheme of the recording device. The fly is placed in front of the laser Doppler vibrometer (LDV) to measure its sound-induced antennal vibration and the ensuing antennal nerve potentials. Tones at frequencies corresponding to the individual best frequency of the antenna were used for sound stimulation. (C) Relative nerve potential amplitudes (top) and antennal displacements (bottom) as functions of the sound intensity. Intensities are presented as sound particle velocities. Blue lines, Hill function fitted to the data from *w*^{1118} flies (top) and line describing the nonlinear behavior of their antennae that results from ciliary motility. The lines are repeated subsequently to facilitate comparisons. Bottom, gray lines depict linear antennal mechanics, as observed when motility is lost. Red arrows highlight differences between *hmw*$^{1/1}$ mutants and *w*^{1118} controls, which include a drop in auditory sensitivity (top) and a reduced antennal nonlinearity that signals a drop in motility ($n = 5$ flies per strain). (D) Hearing thresholds. Thresholds are provided as the sound particle velocities that correspond to 10% of the maximum nerve potentials. Asterisks, significant differences from *w*^{1118} controls ($n = 5$ flies per strain, $p < 0.05$, two-tailed Mann–Whitney *U* test). (E) Mechanical amplification gains deduced from the antennal displacement data in C. Asterisks, significant differences from *w*^{1118} controls ($n = 5$ flies per strain, $p < 0.05$, two-tailed Mann–Whitney *U* test).

mechanical amplification that arises from ciliary motility of auditory chordotonal neurons. In testis, HMW is required for axonemal elongation and integrity. In addition, loss of HMW results in defective sperm individualization associated with altered post-translational tubulin modifications.

hmw is required for acquisition of motile properties in cilia and flagella

HMW is expressed in chordotonal neurons that harbor 9+0 sensory primary cilia presenting dynein-like arms that serve in motility and force generation: motile properties of auditory chordotonal neurons actively amplify sound-induced antennal vibrations (Göpfert and Robert, 2003; Göpfert *et al.*, 2005; Effertz *et al.*, 2011). This amplification is absent from flies carrying mutations in the gene *touch insensitive larvae B* (*tilB*), in which the axonemal dynein-like arms are lost (Kavlie *et al.*, 2010).

Although *hmw* mutant flies have defects in this mechanical amplification, documenting that ciliary motility is impaired; we were not able to detect any structural defects of outer and inner dynein-like arms in *hmw*$^{1/1}$ mutants. Compared to the testis defects, hearing defects were rather mild: judging from the amplification gain, ciliary motility in auditory chordotonal neurons is reduced, but some residual motility remains. Unlike in sperm flagella, we also did not observe axonemal defects in chordotonal neuron cilia, possibly reflecting differences in axoneme length: flagella in *Drosophila* spermatozoa have axonemes that are >1.8 mm long, whereas chordotonal cilia hardly exceed 10 µm in length. Sperm flagella could thus be more sensitive to mechanical constraints and break more easily, simply because of their greater length.

Motility requires elasticity of several components to convert mechanical forces produced by dyneins into axonemal bending. Nexin links play a major role in axonemal elasticity (Lindemann and Lesich, 2010). They have to stretch up to 12 times their resting length without breaking during axonemal motion. Nexin links were not detectable in our electron microscopic analysis of *Drosophila* chordotonal cilia and have not been described in 9+0 primary cilia, and hence it is not possible to conclude on possible defects of the nexin links (or dynein regulatory complexes) in *hmw* mutant flies. Tektins have also been shown to be essential for sperm motility by creating a scaffold allowing deformation and elasticity of the axoneme. Hemingway could be required for the capacity of nexin links to elongate in flagellar axonemes or for the assembly of the tektin scaffold. Mutations in tektin genes affect motility parameters in mouse without affecting axonemal structure (Roy *et al.*, 2007). Of interest, orthologues of *hmw* are found in almost all ciliated species, but we

appeared spotted for both monoglycylation and polyglycylation (Figure 9, D and F). These observations show that HMW deficiency leads to a defective pattern of tubulin glycylation at the onset of spermatid individualization.

DISCUSSION

We identified a novel conserved protein, HMW, required for motile cilia and flagella function. In *Drosophila*, HMW is specifically expressed in motile ciliated cells. In antennae, HMW is required for

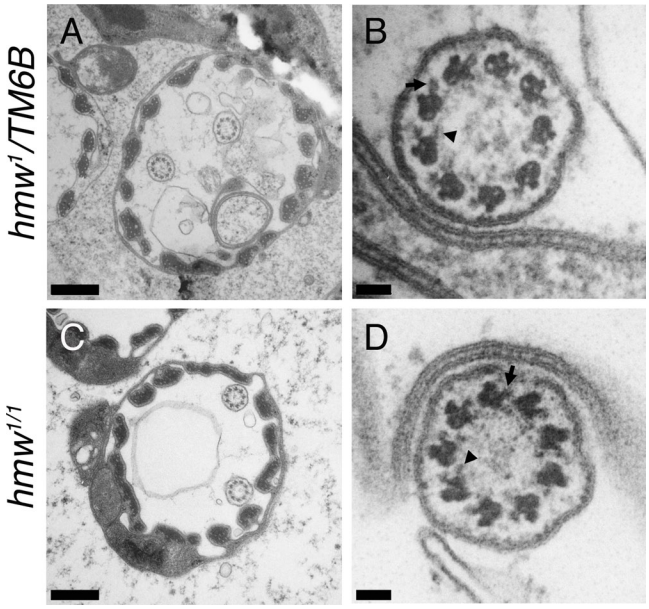

FIGURE 5: Sensory cilia ultrastructure is not affected in *hmw*$^{1/1}$ mutant flies. (A–D) Electron microscopy imaging of transverse sections of Johnston's organ scolopidia. (A, B) *hmw*^{1}/TM6 control flies. (C, D) *hmw*$^{1/1}$ mutant flies. (A, C) An entire scolopidium with two axonemes. No differences could be observed between *hmw*$^{1/1}$ and control scolopidia. Scale bar, 0.5 µm. (B, D) Enlargement of one cilium in a scolopidium. Axonemes are apparently normal in *hmw*$^{1/1}$ flies (D) compared with controls (B), with nine peripheral doublets of microtubules and outer (arrow) and inner (arrowhead) dynein arms. Scale bars, 50 nm.

did not find any *hmw* orthologue in the *Thalassiosira* taxon. *Thalassiosira* have motile axonemes, but only genes encoding outer dynein arm components and not inner dynein arm ones have been found in their genomes (Wickstead and Gull, 2007). If an orthologue of *hemingway* can be found in *Plasmodium*, it is very distant from all other orthologues in other species (e = 4; Wickstead and Gull, 2007). *Plasmodium* does not have the complete set of components of the inner dynein arms. These observations suggest that HMW might have evolved together with inner dynein arm components. Tektin evolution is also correlated with inner dynein arms, and tektins are

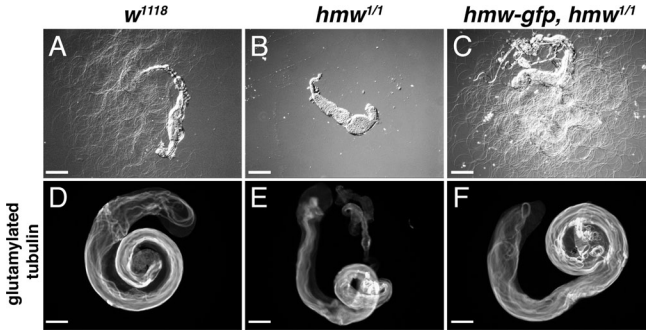

FIGURE 6: *hmw* is required for *Drosophila* spermatogenesis. (A–C) Bright-field images of adult fly seminal vesicles. Control *w*^{1118} (A) and rescue *hmw-gfp, hmw*$^{1/1}$ (C) are filled with mature sperm. Conversely, *hmw*$^{1/1}$ seminal vesicles (B) are empty. (D–F) Whole-mount glutamylated tubulin stainings of *Drosophila* testes showing that flagella are still present in *hmw*$^{1/1}$ mutant testes (E) compared with control (D) or rescue (F) testes. Scale bars, 200 µm.

required for inner dynein arm assembly (Tanaka *et al.*, 2004; Amos, 2008). These observations raise the possibility that HMW works together with tektins for proper function of inner dynein arms.

Because HMW protein appears to be cytoplasmic and not associated with the axoneme in the testis, we are tempted to propose that HMW has an indirect effect on axonemal components involved in motility. One possibility is that HMW could play a chaperone-like function in the assembly of components required for cilia motility and axonemal integrity.

hmw loss of function leads to aberrant tubulin modifications

We showed that the pattern of tubulin glycylation of spermatid axonemes is modified in *hmw*$^{1/1}$ mutant flies. In control flies this pattern is continuous along the spermatid, but appeared in a dotty manner in *hmw*$^{1/1}$ mutant flies. Glycylation is critical during spermiogenesis in *Drosophila*. Indeed, RNAi knockdown of *ttll6b* causes a strong spermatid phenotype that is similar to the one observed in *hmw*$^{1/1}$ flies (Rogowski *et al.*, 2009). Knockdown of *ttll6b* leads to apparently normal early axonemes, but the structure is progressively destabilized and ultimately completely disappears, resulting in male sterility. The function of glycylation is conserved among species. For example, in *T. thermophila* and zebrafish the absence of TTLL3 (orthologue of *ttll6b* in *Drosophila*) provokes ciliary defects such as short cilia or defective peripheral doublet arrangements (Wloga *et al.*, 2009). Hence glycylation defects observed in *hmw*-deficient flies could explain part of the increase in axonemal defects observed during sperm maturation.

In addition, detyrosinated tubulin staining does not disappear at the onset of spermatid individualization in *hmw*$^{1/1}$ flies. Because there is no homologue of tubulin tyrosine ligase in flies, retyrosination likely does not occur, and we favor the hypothesis that glycylation modifications simply cover the epitope for detyrosinated tubulin antibodies. This suggests that in *hmw*$^{1/1}$ testes, glycylation is not as complete as in control ones. These tubulin glycylations defects are only observed after the onset of sperm individualization at a step in which HMW expression is no longer detectable in control *Drosophila* testes. This implies that HMW could either affect tubulin accessibility before the action of TTLL enzyme or act on the switch between the activities of the different tubulin tyrosine ligases at the onset of sperm individualization. Alternatively, HMW could act on other types of tubulin modifications that occur before sperm individualization and are ultimately required for glycylation. It has been shown that tubulin glutamylation may regulate the level of tubulin glycylation (Wloga *et al.*, 2009). In the *hmw*$^{1/1}$ mutant, we did not detect measurable defects in glutamylation level or distribution, but we cannot completely exclude discrete glutamylation defects. Tubulin glycylation defects could also be an indirect consequence of distorted axonemal structure observed in *hmw*$^{1/1}$ testes. Taken together, our observations suggest that HMW plays indirect functions in axonemal assembly and tubulin modifications that ultimately act on cilia motility.

In conclusion, HMW is a novel conserved cytoplasmic component required for the acquisition of motile cilia components. Because motility defects are responsible for primary ciliary dyskinesia in humans, *HMW* is a novel candidate gene that could be involved in this pathology.

MATERIALS AND METHODS

Protein alignments

Protein sequences were obtained from the National Center for Biotechnology Information (NCBI). The conserved domain was defined by best alignment in *Drosophila* species using the Vista Genome

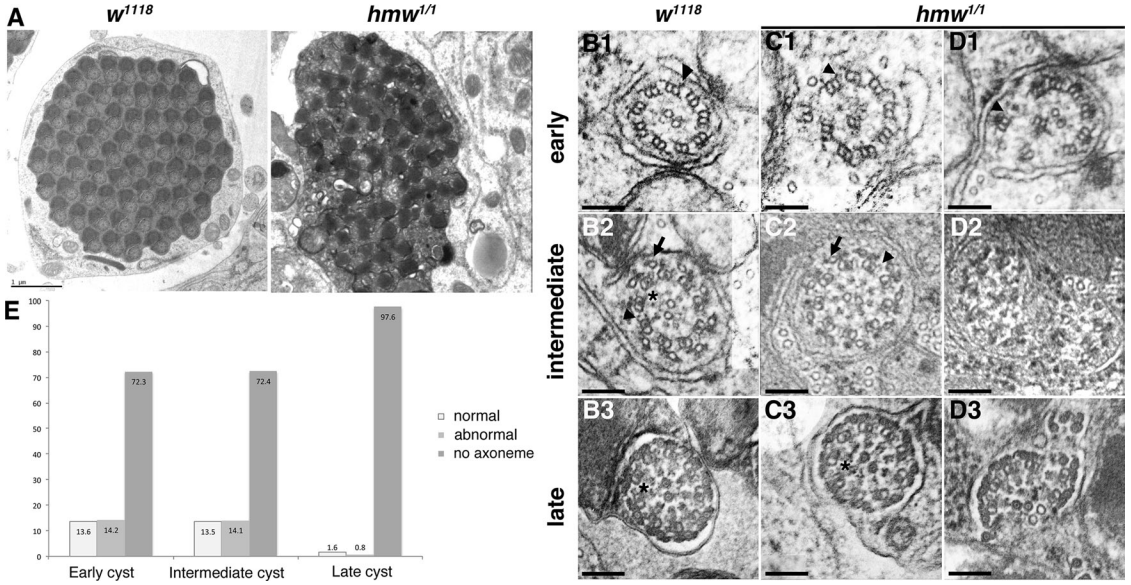

FIGURE 7: *hmw* is involved in flagellar axoneme integrity. (A) Electron microscopy imaging of transverse sections of control or $hmw^{1/1}$ spermatid cysts at late stages of spermatid maturation. Almost no axonemes were observed in mutant cysts, and sperm individualization did not occur. Scale bar, 1 µm. (B–D) Magnification of transverse sections of control (B1-3) or $hmw^{1/1}$ (C1–D3) axonemes at different stages of maturation. (B1) Early control axonemes show a stereotypical 9+2 ultrastructure with outer dynein arms (black arrowheads). (C1, D1) $hmw^{1/1}$ early axonemes are apparently normal in a few situations (unpublished data) but most of the time are broken (72%). The axoneme in D1 shows a more severe phenotype than in C1. In all cases, outer dynein arms could still be observed (arrowheads). (B2) During maturation, accessory components are added on control axonemes, such as accessory microtubules (black arrow), outer and inner dynein arms (black arrowheads), and radial spokes (black star). These structures are also observed in some $hmw^{1/1}$ axonemes (C2), but most appear broken (D2). (B3) Late axonemes are fully matured and show all accessory components in control flies. (C3) A very few mature $hmw^{1/1}$ axonemes are apparently normal. (D3) Most $hmw^{1/1}$ mature axonemes are broken or missing. Scale bars, 100 nm. (E) Quantification of the percentage of spermatids showing axonemal defects in $hmw^{1/1}$-mutant testes ($n = 444$).

Browser (Frazer *et al.*, 2004). Proteins sharing this conserved domain in ciliated species were identified by Position-Specific Iterated BLAST (NCBI). Conserved domains from ciliated species were assessed for best reciprocal hit against *D. melanogaster* domain. Multiple alignments and secondary structure prediction were generated using ClustalW and DSC model with NPS@ (Combet *et al.*, 2000).

Reporter constructs

All primers sequences are described in Supplemental Table S1.

For HMW-GFP, a 4153–base pair fragment including *hmw* coding sequences and upstream regulatory sequences was amplified by PCR on wild-type *Drosophila* genomic DNA with the primers CG7669-pro5/*Sac*II and CG7669-pro3/*Bgl*II. The resulting PCR fragment was cloned into the *Sac*II and *Bam*HI sites of the pW8-GFP plasmid in-frame with the *gfp* sequence. This allows production of an HMW protein fused at its C-terminus with GFP. CBY-Tomato was previously described (Enjolras *et al.*, 2012).

hmw homologous recombination

The *hmw* gene was disrupted by ends-out homologous recombination (Maggert *et al.*, 2008). The left and right arms of the targeting construct were amplified by PCR on genomic DNA of the y[1] w[*]; P{ry[+t7.2] = 70FLP}11 P{v[+t1.8] = 70I-SceI}2B noc[Sco]/CyO, S[2] stock using primers F5′/BsiwI (FS-79), R5′/AscI (FS-80), F3′/SphI (FS-81), and R3′/NotI (FS-116). The resulting construct enabled the deletion of exons 1–4 (Figure 4A). All the coding regions from the cloned 5′ and 3′ homologous fragment were verified by sequencing. Primer sequences, including primers A–H are listed in Supplemental Table S1. Transgenic lines were established by phiC31-mediated germline transformation and used for homologous recombination as described (Maggert *et al.*, 2008).

Fly stocks

Flies were cultured in standard conditions at 25°C.

The following fly strains were constructed in the laboratory: *w; P{hmw::GFP}^{F16}. w; P{hmw::GFP}^{F16}, rfx^{253},e/TM3, P{GAL4-twi.G}$^{2.3}$, P{UAS-2xEGFP}$^{AH2.3}$. w; P{hmw::GFP}^{F16}. w; Bl/CyO; hmw^{1}/TM6B. w; hmw^{1}/TM3, P{GAL4-twi.G}$^{2.3}$, P{UAS-2xEGFP}$^{AH2.3}$. w; Bl/+; P{hmw::GFP}^{F16}, hmw^{1}/TM6B. w; Bl/CyO; P{Cby::Tomato}attP 62E1^{M1F2}/TM6B. w; Bl/CyO; hmw^{1}, P{Cby::Tomato}attP 62E1^{M1F2}/TM6B*.

The w^{1118} allele was obtained from Bloomington *Drosophila* Stock Center, Bloomington, IN.

Hearing phenotype characterization

Eight-day-old adult flies (for each fly strain, $n = 5$) were chosen, and individual best frequencies of their antennal sound receivers were deduced from the power spectra of their mechanical free fluctuations measured by laser Doppler vibrometry (Göpfert *et al.*, 2006; Effertz et al., 2011). To measure sound-induced responses, we exposed flies to pure tones at this antennal best frequency. Sound intensities, measured as the sound particle velocity, were systematically varied between 10^{-3} and 10^{2} mm/s. Resulting antennal displacements were monitored with the laser Doppler vibrometer. Ensuing nerve potentials were recorded extracellularly from the antennal nerve via electrolytically sharpened tungsten electrodes (Effertz *et al.*, 2011).

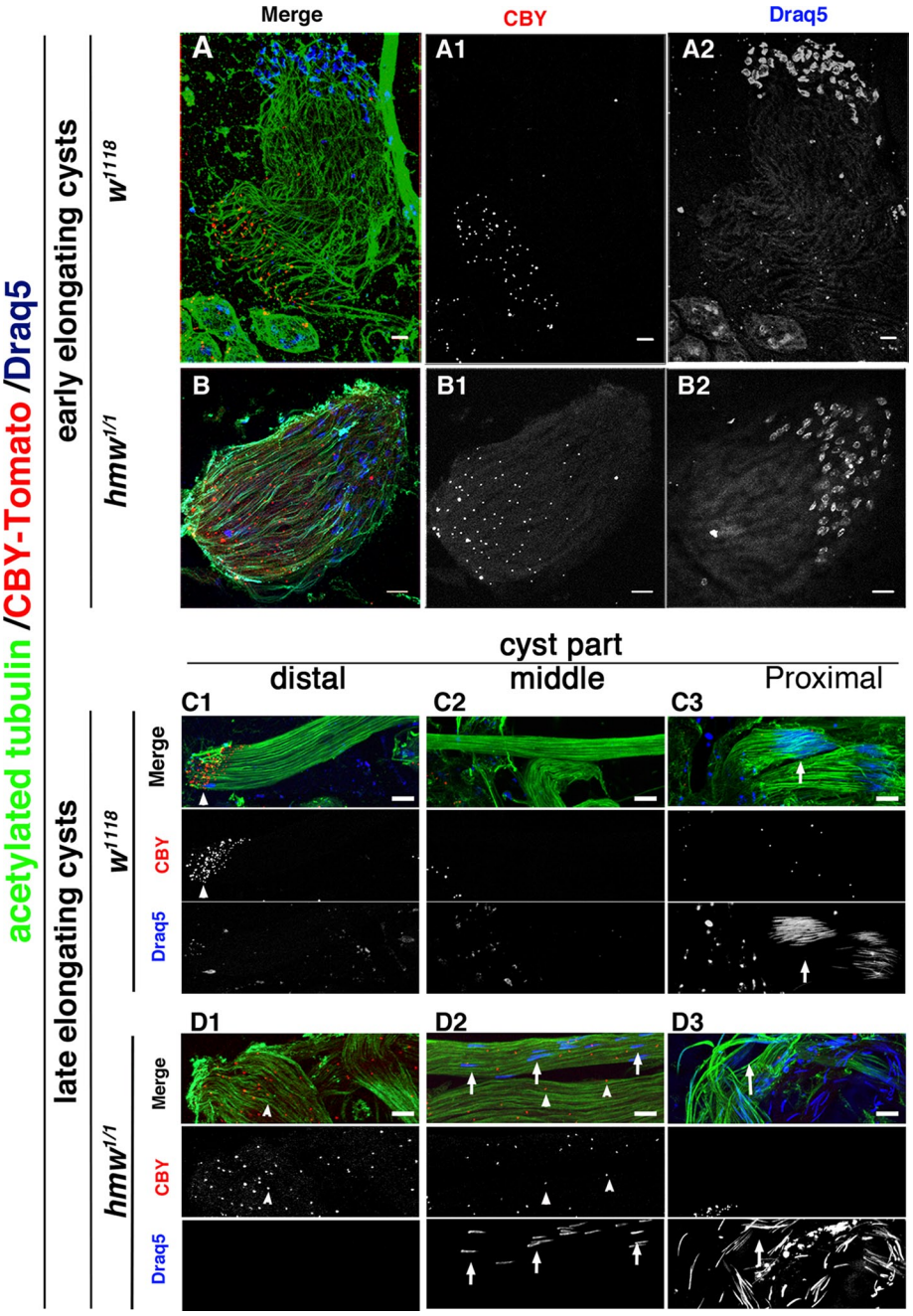

FIGURE 8: *hmw* is required for complete axonemal elongation. Confocal imaging of spermatid cysts labeled for acetylated α-tubulin (green) and the transgenic reporter CBY-Tomato (red). Nuclei are labeled with Draq5 (blue). (A, B) Intermediate-elongating cysts. Single CBY-Tomato (A1, B1) and Draq5 (A2, B2) labelings are presented separately as monochrome images for better contrast. (A) In control cysts, CBY-Tomato staining (red) is clustered at the tip of the axonemes at one pole of the cysts. Nuclei are clustered at the opposite pole. (B) In $hmw^{1/1}$ cysts, CBY staining is found dispersed on one side of the cyst (compare A1 to B1). Similarly, nuclei are less clustered at the opposite pole compared with controls (compare A2 to B2). Scale bars, 10 μm. (C, D) Late-elongating cysts. Top, color merge image. Middle and bottom, CBY-Tomato or Draq5 labeling, respectively, as monochrome images for better contrast. (C1) In control, CBY dots (arrowheads) are clustered at the distal pole of the cyst. (D1) In $hmw^{1/1}$, CBY dots (arrowheads) are dispersed all along the cyst. (C2) In control, we never see nuclei or CBY dots in the middle of the cyst. (D2) In $hmw^{1/1}$, nuclei (arrows) and CBY dots (arrowheads) are detected all along the cyst. (C3) In control, nuclei (arrows) are clustered in the proximal tip of the cyst compared with $hmw^{1/1}$. (D3) With dispersed nuclei. Scale bars, 10 μm.

Mechanical amplification by auditory chordotonal neurons was assessed by plotting antennal displacement against sound intensity. Amplification gains were deduced by comparing normalized antennal displacements at high and low sound intensities (Göpfert *et al.*, 2006). To deduce thresholds of the corresponding nerve responses, their amplitudes were plotted against sound intensity. Thresholds were deduced from Hill fits, using 10% of the maximum as the threshold criterion (Effertz *et al.*, 2011, Senthilan *et al.*, 2012).

Data analysis and statistical data evaluation were performed using Polytec-VIB (Polytec, Waldbronn, Germany), Spike 2 (Cambridge Electronic Design, Cambridge, UK), Excel 2007 (Microsoft, Redmond, WA), and SigmaPlot 10 (Systat Software, San Jose, CA).

Immunostaining

For immunostaining analysis, staged *Drosophila* embryos were treated as described previously (Enjolras *et al.*, 2012). For whole-mount testis preparation, testes were fixed 15 min in 4% paraformaldehyde/phosphate-buffered saline (PBS) 1×, followed by 15-min treatment in PBS 1×, 0.1% Triton X-100, blocked in 3% bovine serum albumin (BSA) in PBS 1×, and incubated with primary antibodies overnight at 4°C. Testes were incubated in secondary antibodies for 2 h at room temperature. For testis squashes, testes (0- to 2-d-old adults) were fixed 20 min at room temperature in PBS 1×/formaldehyde 3.7% and flattened under a coverslip on a microscope slide pretreated with 10% polylysine solution. Slides were quick frozen in liquid nitrogen, and coverslips were removed, fixed in chilled 100% ethanol for 5 min at –20°C, washed 15 min in PBT (PBS 1× containing 0.1% Triton X-100), and blocked for at least 1 h in PBTB (PBT with 3% BSA) at room temperature. Samples were incubated overnight at 4°C in primary antibodies diluted in PBTB and 2 h at room temperature in secondary antibodies in PBS 1×. Testes were mounted in mounting medium (Cytomation DAKO, Glostrup, Denmark).

Antibodies were the following: rabbit anti-GFP (1/500; Molecular Probes, Eugene, OR); rabbit anti–horseradish peroxidase (1/3000; Jackson ImmunoResearch, West Grove, PA); mouse anti-22C10 (1/250; kindly provided by S. Benzer, California Institute of Technology, Pasadena, CA); mouse anti–γ-tubulin (used on testes, 1/500; Sigma-Aldrich, St. Louis, MO); mouse anti–acetylated

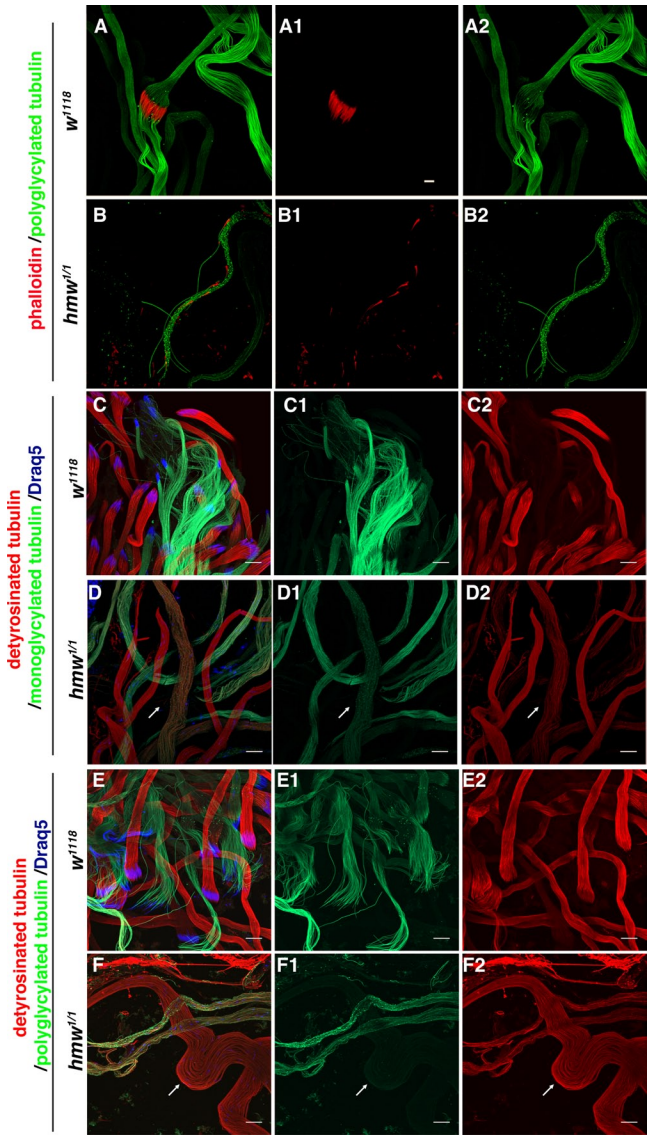

FIGURE 9: *hmw* is required for sperm individualization and tubulin modification in *Drosophila* testis. Immunolabeling of w^{1118} and $hmw^{1/1}$ testis squashes. (A, B) Actin individualization cones are labeled with phalloidin (red), and axonemes are labeled with anti–polyglycylated tubulin antibody (green). (A) Control testes show highly organized individualization complexes compared with $hmw^{1/1}$ testes (B). (A1, B1) Phalloidin staining. (A2, B2) Polyglycylated tubulin staining. (A, B) Merge of the two channels. Scale bars, 10 µm. (C–F) Detyrosinated tubulin is stained with anti–Glu-Tub antibody (red), and nuclei are stained with Draq5 (blue). (C, D) Monoglycylated tubulin is detected with TAP952 antibody (green). (C) w^{1118} axonemes show continuous pattern of glycylation in control and in $hmw^{1/1}$ mutants, with a small overlap of monoglycylation and detyrosination patterns in both situations (D). (E, F) Polyglycylated tubulin is detected with AXO49 antibody (green). (E) w^{1118} testes show continuous pattern of glycylation along the axonemes. Polyglycylations and detyrosinations are mutually exclusive. (F) In $hmw^{1/1}$ testes, axonemes show a dotty pattern of polyglycylations, and simultaneously glycylated and detyrosinated tubulin can be observed (arrow). Scale bars, 20 µm.

α-tubulin (1/500; T6796; Sigma-Aldrich); mouse Axo49 anti–polyglycylated tubulin (1/100; provided by N. Levilliers, Laboratoire de Biologie Cellulaire 4, CNRS, Université Paris-Sud, Orsay, France); mouse Tap952 anti–monoglycylated tubulin (1/10; provided by N. Levilliers); mouse GT335 anti–glutamylated tubulin (1/500; provided by B. Edde, Centre de Recherche de Biochimie Macromoléculaire, CNRS, Montpellier, France); and rabbit anti–Glu-Tub (anti–detyrosinated tubulin; AbCys, Paris, France; ABC0101) antibody (1/500).

Secondary antibodies were diluted at 1/1000: goat anti-mouse Alexa Fluor 488–conjugated and 546–conjugated, and goat anti-rabbit Alexa Fluor 488–conjugated and 555–conjugated (Molecular Probes).

Slides were analyzed at room temperature on a Zeiss Imager Z1 microscope equipped with 5× Plan-Neofluar, 20× Plan-Neofluar (0.5 numerical aperture [NA]). Epifluorescence images were acquired with a charge-coupled device camera (CoolSNAP HQ2; Roper Scientific, Saratosa, FL) and MediaView software (Molecular Devices, Sunnyvale, CA). Confocal stacks were acquired with a confocal microscope (LSM 510 META; Carl Zeiss, Oberkochen, Germany) equipped with 63× Plan-Apochromat (1.4 NA), 40× Plan-Neofluar (1.3 NA), and 25× Plan-Neofluar (0.8 NA) objectives. Image brightness and contrast were adjusted by using ImageJ (National Institutes of Health, Bethesda, MD), and separate panels were assembled with Photoshop CS4 software. Capture times and adjustments were identical for compared images on one figure.

Electron microscopy

For ultrastructural observations, antennae and testes were dissected in PBS 1× and fixed in 2% glutaraldehyde, 0.5% paraformaldehyde, and 0.1 M Na cacodylate (pH 7.4) for 48 h at 4°C. After three washes of 15 min in 0.15 M sodium cacodylate (pH 7.4), samples were post-fixed in 1% OsO4 for 4 h for antennae and 1 h for testes. Samples were then dehydrated through ethanol series and propylene oxide and embedded in Epon medium (Fluka, Buchs, Switzerland). Ultrathin sections were cut on a Leica ultramicrotome. Sections were contrasted in Leica Ultrastainer in aqueous uranyl acetate and lead citrate. Contrasted sections were observed on a Philips CM120 transmission electron microscope.

Seminal vesicle imaging

Two-day-old males were isolated 3 d before imaging. Seminal vesicles were dissected in PBS 1× and squashed on a slide. Slides were analyzed at room temperature on a Zeiss Imager Z1 microscope equipped with 5× Plan-Neofluar.

ACKNOWLEDGMENTS

We thank Jérôme Schmitt and Patricia Morales for *Drosophila* medium and stock maintenance. Electron microscopy was performed at the Center Technologique des Microstructures of the University of Lyon. We thank Gilbert Deléage for help with structural analysis of HMW protein structure. We thank Renata Basto for helpful discussions. This work was supported by grants to B.D. from the Fondation pour la Recherche Médicale (Equipe FRM 2009), the Agence National de la Recherche (Ciliopath-X), and the Région Rhône-Alpes (Cible 2008), as well as by grants to M.C.G. from the Bundesministeriums für Bildung und Forschung Göttingen Bernstein Center (A1) and the German Science Foundation (SFB 889, C2). F.S. and D.P. were supported by doctoral fellowships from the Région Rhône-Alpes and the German National Academic Foundation, respectively. J.V. is supported by a doctoral fellowship from University of Lyon 1.

REFERENCES

Amos LA (2008). The tektin family of microtubule-stabilizing proteins. Genome Biol 9, 229.

Avidor-Reiss T, Maer A, Koundakjian E, Polyanovsky A, Keil T, Subramaniam S, Zuker C (2004). Decoding cilia function: defining specialized genes required for compartmentalized cilia biogenesis. Cell 117, 527–539.

Baron D, Ralston K, Kabututu Z, Hill K (2007). Functional genomics in *Trypanosoma brucei* identifies evolutionarily conserved components of motile flagella. J Cell Sci 120, 478–491.

Bonnafe E *et al*. (2004). The transcription factor RFX3 directs nodal cilium development and left-right asymmetry specification. Mol Cell Biol 24, 4417–4427.

Bré MH *et al*. (1996). Axonemal tubulin polyglycylation probed with two monoclonal antibodies: widespread evolutionary distribution, appearance during spermatozoan maturation and possible function in motility. J Cell Sci 109, 727–738.

Combet C, Blanchet C, Geourjon C, Deléage G (2000). NPS@: network protein sequence analysis. Trends Biochem Sci 25, 147–150.

Drummond IA (2012). Cilia functions in development. Curr Opin Cell Biol 24, 24–30.

Dubruille R, Laurençon A, Vandaele C, Shishido E, Coulon-Bublex M, Swoboda P, Couble P, Kernan M, Durand B (2002). *Drosophila* regulatory factor X is necessary for ciliated sensory neuron differentiation. Development 129, 5487–5498.

Effertz T, Wiek R, Göpfert MC (2011). NompC TRP channel is essential for *Drosophila* sound receptor function. Curr Biol 21, 592–597.

Enjolras C, Thomas J, Chhin B, Cortier E, Duteyrat JL, Soulavie F, Kernan MJ, Laurencon A, Durand B (2012). *Drosophila* chibby is required for basal body formation and ciliogenesis but not for Wg signaling. J Cell Biol 197, 313–325.

Frazer K, Pachter L, Poliakov A, Rubin E, Dubchak I (2004). VISTA: computational tools for comparative genomics. Nucleic Acids Res 32, W273–W279.

Gagnon C, White D, Cosson J, Huitorel P, Edde B, Desbruyeres E, Paturle-Lafanechère L, Multigner L, Job D, Cibert C (1996). The polyglutamylated lateral chain of alpha-tubulin plays a key role in flagellar motility. J Cell Sci 109, 1545–1553.

Göpfert MC, Albert JT, Nadrowski B, Kamikouchi A (2006). Specification of auditory sensitivity by *Drosophila* TRP channels. Nat Neurosci 9, 999–1000.

Göpfert MC, Humphris ADL, Albert JT, Robert D, Hendrich O (2005). Power gain exhibited by motile mechanosensory neurons in *Drosophila* ears. Proc Natl Acad Sci USA 102, 325–330.

Göpfert MC, Robert D (2003). Motion generation by *Drosophila* mechanosensory neurons. Proc Natl Acad Sci USA 100, 5514–5519.

Hildebrandt F, Benzing T, Katsanis N (2011). Ciliopathies. N Engl J Med 364, 1533–1543.

Hoyle HD, Turner FR, Raff EC (2008). Axoneme-dependent tubulin modifications in singlet microtubules of the *Drosophila* sperm tail. Cell Motil Cytoskeleton 65, 295–313.

Ikegami K, Sato S, Nakamura K, Ostrowski LE, Setou M (2010). Tubulin polyglutamylation is essential for airway ciliary function through the regulation of beating asymmetry. Proc Natl Acad Sci USA 107, 10490–10495.

Jarman A, Grau Y, Jan L, Jan Y (1993). atonal is a proneural gene that directs chordotonal organ formation in the *Drosophila* peripheral nervous system. Cell 73, 1307–1321.

Kamikouchi A, Inagaki HK, Effertz T, Hendrich O, Fiala A, Göpfert MC, Ito K (2009). The neural basis of *Drosophila* gravity-sensing and hearing. Nature 458, 165–171.

Kamikouchi A, Shimada T, Ito K (2006). Comprehensive classification of the auditory sensory projections in the brain of the fruit fly *Drosophila melanogaster*. J Comp Neurol 499, 317–356.

Kavlie RG, Kernan MJ, Eberl DF (2010). Hearing in *Drosophila* requires TilB, a conserved protein associated with ciliary motility. Genetics 185, 177–188.

King RD, Saqi M, Sayle R, Sternberg MJ (1997). DSC: public domain protein secondary structure predication. Comput Appl Biosci 13, 473–474.

Kubo T, Yanagisawa H-A, Yagi T, Hirono M, Kamiya R (2010). Tubulin polyglutamylation regulates axonemal motility by modulating activities of inner-arm dyneins. Curr Biol 20, 441–445.

Laurençon A, Dubruille R, Efimenko E, Grenier G, Bissett R, Cortier E, Rolland V, Swoboda P, Durand B (2007). Identification of novel regulatory factor X (RFX) target genes by comparative genomics in *Drosophila* species. Genome Biol 8, R195.

Lindemann CB, Lesich KA (2010). Flagellar and ciliary beating: the proven and the possible. J Cell Sci 123, 519–528.

Maggert KA, Gong WJ, Golic KG (2008). Methods for homologous recombination in *Drosophila*. Methods Mol Biol 420, 155–174.

McGrath J, Brueckner M (2003). Cilia are at the heart of vertebrate left-right asymmetry. Curr Opin Genet Dev 13, 385–392.

Merchant SS *et al*. (2007). The *Chlamydomonas* genome reveals the evolution of key animal and plant functions. Science 318, 245–250.

O'Hagan R, Piasecki BP, Silva M, Phirke P, Nguyen KCQ, Hall DH, Swoboda P, Barr MM (2011). The tubulin deglutamylase CCPP-1 regulates the function and stability of sensory cilia in *C. elegans*. Curr Biol 21, 1685–1694.

Ostrowski L, Blackburn K, Radde K, Moyer M, Schlatzer D, Moseley A, Boucher R (2002). A proteomic analysis of human cilia: identification of novel components. Mol Cell Proteomics 1, 451–465.

Rogowski K *et al*. (2009). Evolutionary divergence of enzymatic mechanisms for posttranslational polyglycylation. Cell 137, 1076–1087.

Rogowski K *et al*. (2010). A family of protein-deglutamylating enzymes associated with neurodegeneration. Cell 143, 564–578.

Roy A, Lin YN, Agno JE, DeMayo FJ, Matzuk MM (2007). Absence of tektin 4 causes asthenozoospermia and subfertility in male mice. FASEB J 21, 1013–1025.

Satir P (1989). The role of axonemal components in ciliary motility. Comp Biochem Physiol A Comp Physiol 94, 351–357.

Senthilan PR, Piepenbrock D, Ovezmyradov G, Nadrowski B, Bechstedt S, Pauls S, Winkler M, Möbius W, Howard J, Göpfert MC (2012). *Drosophila* auditory organ genes and genetic hearing defects. Cell 150, 1042–1054.

Suryavanshi S, Eddé B, Fox LA, Guerrero S, Hard R, Hennessey T, Kabi A, Malison D, Pennock D, Sale WS (2010). Tubulin glutamylation regulates ciliary motility by altering inner dynein arm activity. Curr Biol 20, 435–440.

Swoboda P, Adler HT, Thomas JH (2000). The RFX-type transcription factor DAF-19 regulates sensory neuron cilium formation in *C. elegans*. Mol Cell 5, 411–421.

Tanaka H, Iguchi N, Toyama Y, Kitamura K, Takahashi T, Kaseda K, Maekawa M, Nishimune Y (2004). Mice deficient in the axonemal protein tektin-t exhibit male infertility and immotile-cilium syndrome due to impaired inner arm dynein function. Mol Cell Biol 24, 7958–7964.

Thomas J, Morle L, Soulavie F, Laurencon A, Sagnol S, Durand B (2010). Transcriptional control of genes involved in ciliogenesis: a first step in making cilia. Biol Cell 102, 499–513.

Wickstead B, Gull K (2007). Dyneins across eukaryotes: a comparative genomic analysis. Traffic 8, 1708–1721.

Wloga D, Gaertig J (2010). Post-translational modifications of microtubules. J Cell Sci 124, 154–154.

Wloga D, Webster DM, Rogowski K, Bré M-H, Levilliers N, Jerka-Dziadosz M, Janke C, Dougan ST, Gaertig J (2009). TTLL3 is a tubulin glycine ligase that regulates the assembly of cilia. Dev Cell 16, 867–876.

Wolff A, de Néchaud B, Chillet D, Mazarguil H, Desbruyeres E, Audebert S, Edde B, Gros F, Denoulet P (1992). Distribution of glutamylated alpha and beta-tubulin in mouse tissues using a specific monoclonal antibody, GT335. Eur J Cell Biol 59, 425–432.